(see [2], [3]) the bifurcations occur most clearly when $Ka \approx 0.3 - 0.5$. Therefore, the interpretation of microwave data of $\Delta T_B(Ka, N)$ in the range $0 \leq Ka \leq 0.5$ is based on the one-dimensional model (4). If $Ka \sim 0.5-1.0$ we can consider the microwave model in which the free surface has the form, for example,

$$\xi(x,y) = \sum_{n=0}^{\alpha} \sum_{m=0}^{\alpha} A_{n,m}(K_x, K_y) \cos(nK_x x + \varphi_n) \cos(mK_y y) \tag{6}$$

where K_x and K_y are the wave numbers. In this case, the cross polarized contribution to microwave emission of the large-scale surface must be taken into account, a problem which requires special calculations.

ACKNOWLEDGMENT

The authors wish to thank Dr. J. Doviak and Dr. A. Stogryn for their helpful comments.

REFERENCES

[1] H. C. Yuen and B. M. Lake, "Nonlinear dynamics of deep-water gravity waves," *Adv. Appl. Mech.*, vol. 22. New York: Academic Press, 1982.
[2] V. A. Ilyin, A. A. Naumov, V. Yu. Raiser, *et al.*, "Influence of short gravity waves on the thermal radio-radiation of the water surface," *Izvestiya of Academy of Sciences USSR, Atmospheric and oceanic physics*, vol. 21, no. 1, pp. 83–89, 1985.
[3] V. A. Ilyin, M. S. Kamenetskaya, V. Yu. Raiser, *et al.*, "Microwave study of surface nonlinear waves," *Izvestiya of Academy of Sciences USSR, Atmospheric and Oceanic Physics*, vol. 24, no. 6, pp. 640–646, 1988.
[4] F. G. Bass and I. M. Fuks, *The Scattering of Waves from Random Surface.* Moscow: Nauka, 1974.
[5] H. Lamb, *Hydrodynamics.* New York: Dover Publications, 1945.
[6] A. Stogryn, "The apparent temperature of the sea at microwave frequencies," *IEEE Trans. Antennas Prop.*, vol. AP-15, pp. 278–286, 1967.
[7] M.-Y. Su, "Three-dimensional deep-water waves. Part 1. Experimental measurement of skew and symmetric wave patterns," *J. Fluid Mech.*, vol. 124, no. 1, pp. 73–108, 1982.

SAR Ocean Image Decomposition Using the Gabor Expansion

J. G. Teti, Jr. and H. N. Kritikos

***Abstract*—This paper demonstrates the utility of the Gabor expansion as a new tool in geophysical research. The Gabor expansion provides good time-frequency (or space-wavenumber) localization and is ideally suited to represent nonstationary processes. The properties of this tool are demonstrated by expanding an FM-chirp waveform, and azimuth cuts taken from two different SAR ocean images. The effects of filtering in Gabor phase space are also investigated.**

Manuscript received April 3, 1991; revised July 17, 1991.

J. G. Teti and H. N. Kritikos are with the Moore School of Electrical Engineering, University of Pennsylvania, Philadelphia, PA 19104. J. G. Teti, Jr. was on leave under the Ph.D. Fellowship Program from the Naval Air Development Center, Warminster, PA.

IEEE Log Number 9103406.

I. INTRODUCTION

The advantages of identifying and/or constructing signals or functions with both time and frequency localization has been of interest to the remote sensing community. Such examples include SAR imaging of a nonuniform ocean [5], transient analysis of lightning [7], etc.. An expansion having these properties can provide a numerically efficient representation of dominant image features. Bastiaans [1] is perhaps the earliest researcher to give recent attention to the expansion of a signal into Gaussian elementary signals, a concept first discussed by Gabor [4]. Bastiaans computed the bi-orthogonal basis corresponding to the Gabor function which stimulated renewed interest in the use of the Gabor expansion [6]. The initial attempts to expand a waveform were found to have poor convergence because of numerical instability caused by singularities present in the solution [3]. Daubechies [3] has successfully addressed this problem by considering an oversampled lattice in phase space. She has also laid out much of the mathematical groundwork needed to carry out such an expansion and her work forms a basis from which the tools utilized in this paper have evolved. The understanding of a "frame" is perhaps the key concept required to appreciate the use of these tools and a brief development is presented following Daubechies [3].

II. MATHEMATICAL PRELIMINARIES

A. The Gabor Expansion

To properly define a frame it is necessary to begin with functions f defined on the Banach space $L^2(\mathbb{R})$. The Banach space $L^2(\mathbb{R})$ is the normed vector space defined as

$$L^2(\mathbb{R}) = \left\{ f : \int_{\mathbb{R}} |f(x)|^2 dx < \infty \right\} \tag{1}$$

with the norm

$$\|f\|_2 = \left(\int_{\mathbb{R}} |f(x)|^2 dx \right)^{\frac{1}{2}} \tag{2}$$

where the subscript 2 is typically omitted. The Hilbert space $\mathcal{H}$ is an inner product space in which every Cauchy sequence $\{\Psi_n\}$ converges, and is also a Banach space. A sequence $\{\Psi_n\}$ in a Hilbert space $\mathcal{H}$ defines a frame if there exist numbers $A, B > 0$ such that

$$\forall\, f \in \mathcal{H}, \quad A\|f\|^2 \leq \sum_n |< \Psi_n, f >|^2 \leq B\|f\|^2 \tag{3}$$

where the numbers A, B represent the frame bounds. If $A = B$ the frame is tight; if $A \approx B$ the frame is said to be snug. Furthermore, a frame is exact if the deletion of any single frame element causes the remaining set of elements to no longer represent a frame. An exact frame is an irreducible set $\{\Psi_n\}$ which forms a sequence that satisfies (3). This statement is somewhat analogous to the requirement of completeness for an orthonormal basis. A complete orthonormal basis is an exact frame; however, the converse is not true in general. Following Daubechies [3], from (3) a frame operator $\mathcal{T}$ and its adjoint $\mathcal{T}^*$ may be defined where

$$A\mathbf{1} \leq \mathcal{T}^*\mathcal{T} \leq \mathrm{B}\mathbf{1} \tag{4}$$

and since $A, B > 0$, the inverse of this operator must exist and satisfy the relation

$$\frac{1}{B}\mathbf{1} \leq (\mathcal{T}^*\mathcal{T})^{-1} \leq \frac{1}{A}\mathbf{1} \tag{5}$$

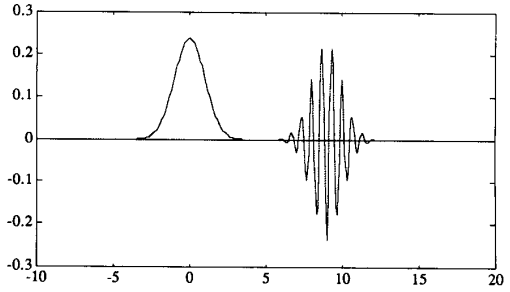

(a)

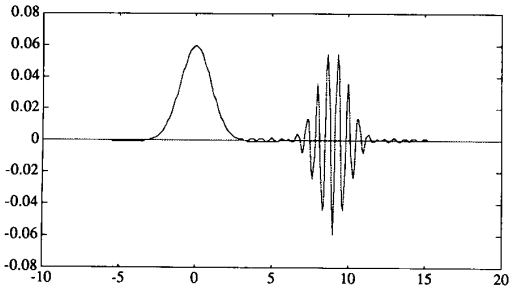

(b)

Fig. 1. (a) Re[g_{mn}] = g_{00} and Re[g_{69}] shown. (b) Re[$\tilde{g}_{mn}$] = $\tilde{g}_{00}$ and Re[$\tilde{g}_{69}$] shown.

where $\mathbf{1}$ is the identity operator. With

$$\tilde{\Psi}_n \triangleq (T^*T)^{-1}\Psi_n = \mathbb{T}^{-1}\Psi_n \tag{6}$$

$\{\tilde{\Psi}_n\}$ constitutes a "dual" or "complimentary" frame with frame bounds A^{-1}, $B^{-1} > 0$ and the operator $\mathbb{T} = T^*T$ is found to be

$$\mathbb{T} = \sum_{n=-\infty}^{\infty} \Psi_n < \Psi_n, \cdot > . \tag{7}$$

With $\{\Psi_n\}$ and $\{\tilde{\Psi}_n\}$ satisfying the prescribed conditions then

$$\forall f \in \mathcal{H}, \quad f = \sum_n \tilde{\Psi}_n < \Psi_n, f > . \tag{8}$$

Note that in a special case $\{\tilde{\Psi}_n\}$ may represent a bi-orthogonal basis. To use (8) it is necessary to acquire the dual frame which from (4) can be found with the series

$$\tilde{\Psi}_n = \frac{2}{A+B} \sum_{k=0}^{\infty} \left(\mathbf{1} - \frac{2}{A+B}\mathbb{T}\right)^k \Psi_n \tag{9}$$

along with good estimates of the frame bounds A and B. The series in (9) is guaranteed to converge by virtue of its development and the tighter the frame the faster the convergence [3].

In the special case of the Gabor expansion the frame elements are generated from the translation and modulation relation

$$g_{pq}(x) = g(x-q)e^{ipx} \tag{10}$$

and the "mother" function

$$g(x) = \pi^{-\frac{1}{4}} e^{-\frac{x^2}{2}}. \tag{11}$$

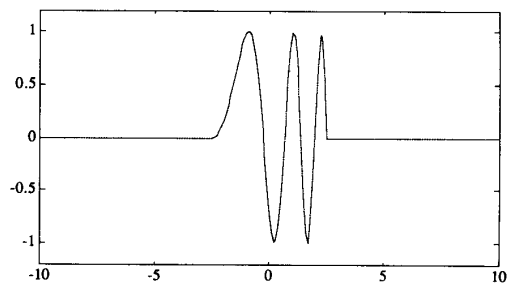

(a)

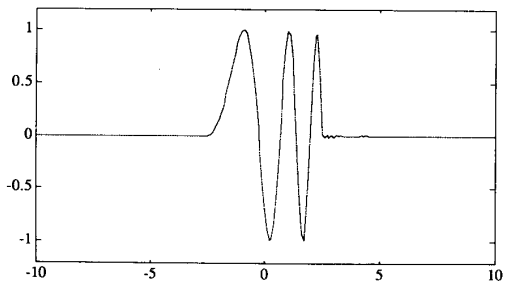

(b)

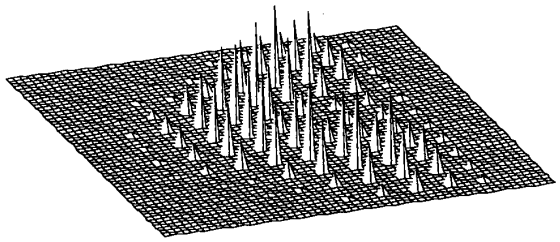

(c)

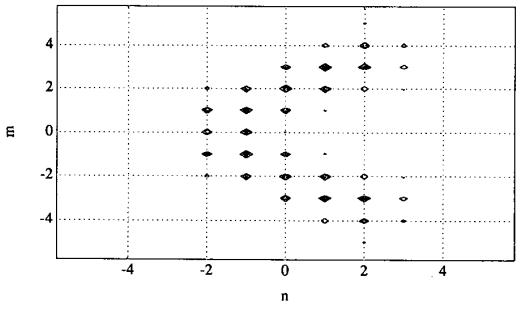

(d)

Fig. 2. (a) Original FM-chirp waveform. (b) Reconstructed FM-chirp waveform. (c) Gabor phase space for FM-chirp waveform. (d) Gabor phase space contour for FM-chirp waveform.

Similarly, once the dual frame mother function is known, all the dual frame elements can be generated from the translation and modulation

(a)

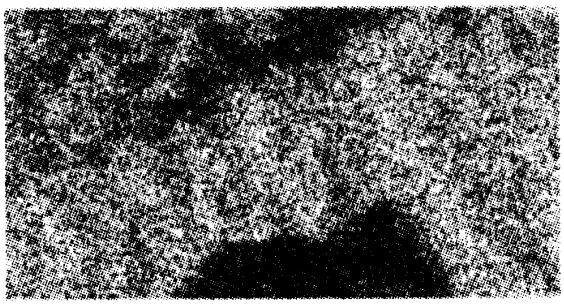

(b)

Fig. 3. (a) SAR image of ship at *X*-band, *VV*-polarization (see text). (b) SAR image of ship wake at *C*-Band, *VV*-polarization (see text).

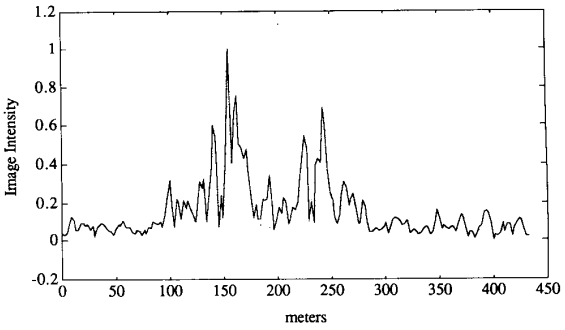

(a)

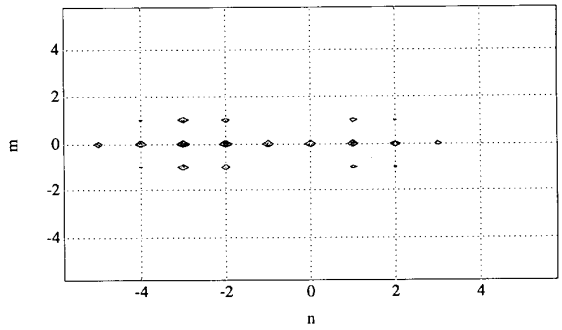

(b)

Fig. 4. (a) SAR ship image azimuth cut (original and reconstructed). (b) Gabor phase space contour of SAR ship image azimuth cut.

relation

$$\tilde{g}_{pq}(x) = \tilde{g}(x-q)e^{ipx}. \tag{12}$$

If the indexes of (p, q) are restricted to the discrete sublattice (mp_o, nq_o) with $p_o, q_o > 0$, $p_o q_o < 2\pi$, the validity of (8) is maintained. Note that the case $p_o q_o = 2\pi$ corresponds to the Nyquist sampling criteria, and causes singularities in (9) which lead to poor convergence properties. Furthermore, $\{g_{mn}\}$ will no longer constitute a frame for this limiting case [3]. Consequently, some oversampling is required for useful application. Daubechies [3] has estimated the frame bounds A and B quite accurately for a range of lattice parameters p_o, q_o from which particular values were chosen for use in this work. Specifically, a snug frame is used with frame bounds $A = 3.854$ and $B = 4.147$, and oversampling $p_o q_o = \pi/2$; $q_o = 1$. Selected elements from the Gabor frame and the dual Gabor frame corresponding to these parameters are illustrated in Figs. 1(a), (b).

B. FM Chirp Waveform

Figs. 2(a)–(d) show the Gabor expansion representation of a pulse modulated FM-chirp waveform. Fig. 2(a) shows the original waveform, and Fig. 2(b) shows the Gabor expansion of the original waveform. The reconstruction uses 1369 terms to yield 99.97% of the original waveform power. Clearly, less terms are permissive for "good" reconstruction. Note the presence of the Gibb's phenomena primarily on the high frequency side of the waveform. Figs. 2(c), (d) show the Gabor phase space representation of this waveform illustrating the dominant coefficients produced by the inner product in (8). The "pluming" structure best shown in Fig. 2(d) is an interesting result because it illustrates the time evolution of the waveform's frequency content.

III. SAR Ocean Image Decomposition

In this section the Gabor expansion representation is investigated for azimuth cuts of the two SAR ocean images shown in Figs. 3(a), (b). The images were provided by the Naval Air Development Center (NADC) SAR image processing facility from experiments conducted off the east coast of the U. S. during the summer and fall of 1988. The image shown in Fig. 3(a) was formed from *X*-band data collected at *VV* polarization. The bright central region is a ship target of opportunity over which an azimuth cut was chosen for expansion. The image shown in Fig. 3(b) was formed from *C*-band data collected at *VV* polarization. The dominant features represent a ship wake torn from conflicting velocity fields present on the ocean surface. The lower edge contains high image intensity activity over which a second azimuth cut was chosen for expansion. For both images the pixel sizes are (range, azimuth) = (2.5, 2.16) m.

A. Representation and Reconstruction

The ship image azimuth cut selected from Fig. 3(a) along with the corresponding Gabor expansion representation is shown in Fig. 4(a) for the parameters given in Section II.A. The reconstructed waveform superimposed as a dotted line over the original uses 1681 terms to yield 99.79% of the original power. Fig. 4(b) shows a subsection of the corresponding Gabor phase space, illustrating the localization of the dominant coefficients produced by the inner product in (8).

The ship wake image azimuth cut selected from Fig. 3(b) along with the corresponding Gabor expansion representation is shown in Fig. 5(a) for the parameters given in Section II.A. The reconstructed waveform superimposed as a dotted line over the original uses

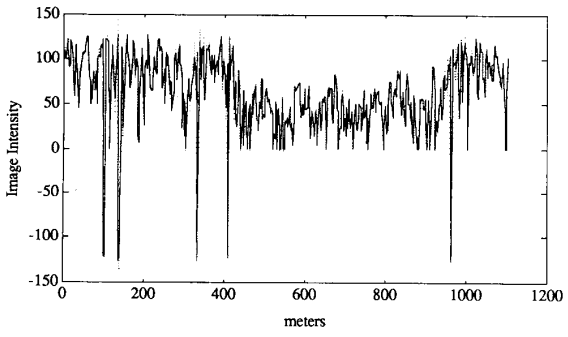

(a)

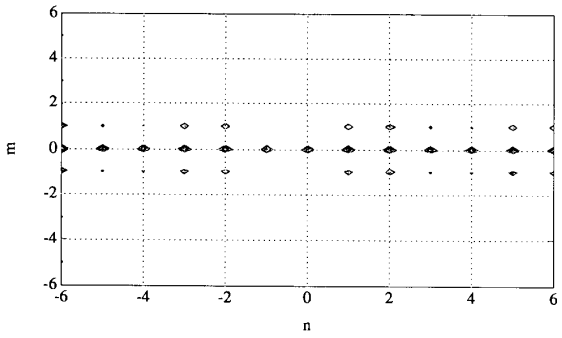

(b)

Fig. 5. (a) SAR ship wake image azimuth cut (original and reconstructed). (b) Gabor phase space contour of SAR ship wake image azimuth cut.

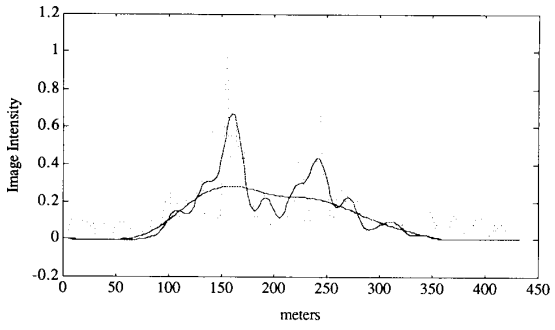

(a)

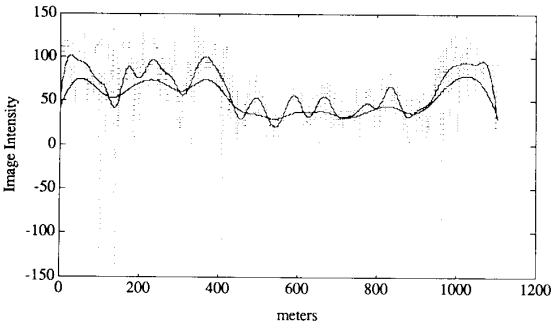

(b)

Fig. 6. (a) Filtered SAR ship image azimuth cut (see text). (b) filtered SAR ship wake image azimuth cut (see text).

2849 terms to yield 98.61% of the original power. Note that in this case the azimuth cut expanded is > 2.5 times the length of the azimuth cut for the ship in Fig. 4. Fig. 5(b) shows a subsection of the corresponding Gabor phase space, illustrating the localization of the dominant coefficients produced by the inner product in (8).

B. Filtered Reconstruction

Using the information provided by the Gabor phase space representation shown in Figs. 4(b) and 5(b), the image reconstruction can easily be limited to the dominant frame contributions. With this in mind and first referring to Fig. 4(b), two filtered image cuts of the ship response have been constructed and are shown in Fig. 6(a). The DC-only response $\{(m,n) = (0,-5\ldots5)\}$, and the DC-plus first three harmonics response $\{(m,n) = (-3\ldots3,-5\ldots5)\}$ are shown superimposed over the original expanded azimuth cut of Fig. 4(a). The DC-only filtered cut uses 11 terms and represents 43.94% of the original waveform power, and the DC-plus first three harmonics filtered cut uses 77 terms and represents 79.11% of the original waveform power. In both cases the ship envelope is preserved and the desired level of detail can be selected based on the application.

Referring to Fig. 5(b), two filtered image cuts of the ship wake response have been constructed and are shown in Fig. 6(b). The DC-only response $\{(m,n) = (0,-38\ldots38)\}$, and the DC-plus first harmonic response $\{(m,n) = (-1\ldots1,-38\ldots38)\}$ are shown superimposed over the original expanded azimuth cut of Fig. 5(a). The DC-only filtered cut uses 77 terms and represents 52.92% of the original waveform power, and the DC-plus first harmonic filtered cut uses 231 terms and represents 79.11% of the original waveform power. As in the filtered ship azimuth cut, the wake scattering envelope is also preserved in both cases.

IV. Conclusion

The Gabor expansion of SAR returns has been investigated and shown to provide an alternate representation of localized space-wavenumber information. This effort has demonstrated that a simple and numerically tractable procedure for the analysis of geophysical data is available through the use of the dual frame. After numerically constructing the dual frame mother function $\tilde{g}_{00}(x)$, the formulation of the dual frame is straightforward through translation and modulation.

The phase space representation of a signal is very important in illustrating the space or time evolution of a waveform's frequency content. It is analogous to the sliding window Fourier transform in that the window position and frequency content correspond to the concept of the phase space lattice (mp_o, nq_o) density inherent in the Gabor frame. The Gabor expansion and ultimate choice of the p_oq_o product produce a unique phase space waveform signature which is simultaneously localized in both space and frequency.

To demonstrate the physical insight afforded by the Gabor phase space, an FM-chirp waveform was expanded. Fig. 2(c), (d) shows a

distinct "pluming" of the coefficients illustrating the time evolution of the waveform's frequency content.

Filtering in Gabor space also provides a useful tool for gracefully reducing, not "cropping", high frequency information and also preserves image features. This has been clearly shown for the SAR image cuts that have been analyzed. The filtering is successful at removing speckle while still preserving the scattering envelope of the ship and wake features.

Classical tools for analysis are not that unlike the tools used here. The Gabor expansion, in a sense, represents a limiting case of the sliding window Fourier transform for optimum time-frequency or space-wavenumber localization. The cost paid for the optimum localization is oversampling and perhaps higher computational overhead resulting from the construction of the dual frame. The increase in the sampling rate results in tighter frames that allow the determination of the dual frame from the series in (9) to converge more quickly. From these considerations the ultimate utility of the Gabor expansion, when compared to classical techniques, is application driven. The Gabor frame is only one of the many frame representations available for waveform analysis. The literature is rich with other candidates known as wavelets which offer a nonuniform lattice in phase space. These candidates will be investigated in future work.

ACKNOWLEDGMENT

The authors thank S. Krasznay of NADC and F. Ilsemann of JJM Systems, Inc. for their assistance in obtaining the SAR imagery from the NADC SAR image processing facility.

REFERENCES

[1] M. J. Bastiaans, "Gabor's expansion of a signal into Gaussian elementary signals," *Proc. IEEE*, vol. 68, pp. 538–539, April 1980.

[2] J. M. Combes, A. Grossmann, and Ph. Tchamitchian, Eds., *Wavelets*. Berlin, Heidelberg: Springer-Verlag, 1990.

[3] I. Daubechies, "The wavelet transform, time frequency localization and signal analysis," *IEEE Trans. Inform. Theory*, vol. 36, pp. 961–1005, Sept. 1990.

[4] D. Gabor, "Theory of communication," *J. IEE (London)*, vol. 93, no. 3, pp. 429–457, Nov. 1946.

[5] K. Hasselmann, R. K. Raney, W. J. Plant, W. Alpers, R. A. Schuchman, D. R. Lyzenga C. L. Rufenach, and M. J. Tucker, "Theory of synthetic aperture radar ocean wave imaging: a MARSEN view," *J. Geophys. Res.*, vol. 90, no. C3, pp. 4659–4686, 1985.

[6] H. N. Kritikos and P. T. Farnum, "Approximate evaluations of Gabor expansions, *IEEE Trans. Syst., Man, Cybern.*, vol. SMC-17, pp. 978–981, Nov.–Dec. 1987.

[7] V. Mazur, D. S. Zrnic, and W. D. Rust, "Lightning channel properties determined with a vertically pointing Doppler radar ," *J. Geophys. Res.*, vol. 90, no. D4, pp. 6165–6174, 1985.